

## Supporting Information

### **Biosynthetic neoantigen displayed on bacteria derived vesicles elicit systemic antitumor immunity**

Fanqiang Meng<sup>1,#</sup>, Liyan Li<sup>1,#</sup>, Zhirang Zhang<sup>1,#</sup>, Zhongda Lin<sup>1</sup>, Jinxie Zhang<sup>4</sup>, Xiao Song<sup>1</sup>, Tianyuan Xue<sup>1</sup>, Chenyang Xing<sup>5</sup>, Xin Liang<sup>2,3 \*</sup>, Xudong Zhang<sup>1,\*</sup>

1. Department of Pharmacology, Molecular Cancer Research Center, School of Medicine, Shenzhen Campus of Sun Yat-sen University, Sun Yat-sen University, No. 66, Gongchang Road, Guangming District, Shenzhen, Guangdong, 518107, P.R. China.

2. Guangdong Provincial Key Laboratory of Medical Molecular Diagnostics, Key Laboratory of Stem Cell and Regenerative Tissue Engineering, School of Basic Medical Sciences, Guangdong Medical University, Dongguan 523808, P.R. China.

3. University of Chinese Academy of Sciences-Shenzhen Hospital, Shenzhen 518000, P. R. China.

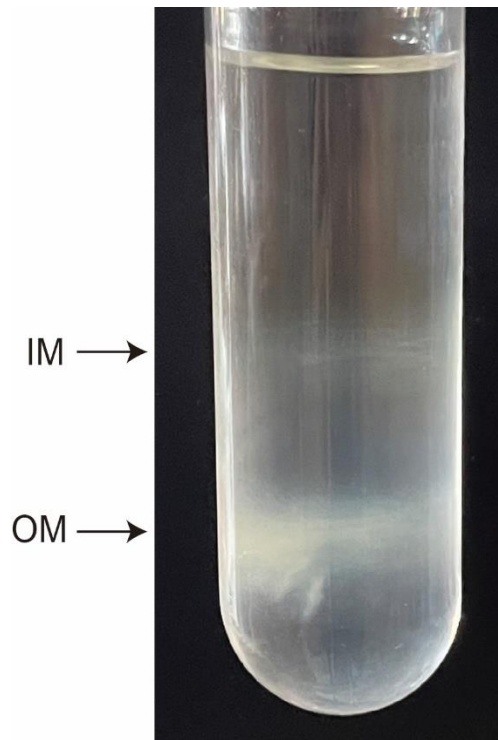
4. School of Pharmaceutical Sciences (Shenzhen), Shenzhen Campus of Sun Yat-Sen University, Shenzhen, Guangdong, 518107, P.R. China.

5. Key Laboratory of Optoelectronic Devices and Systems of Ministry of Education, College of Physics and Optoelectronic Engineering Shenzhen University, Shenzhen, 518060, P. R. China.

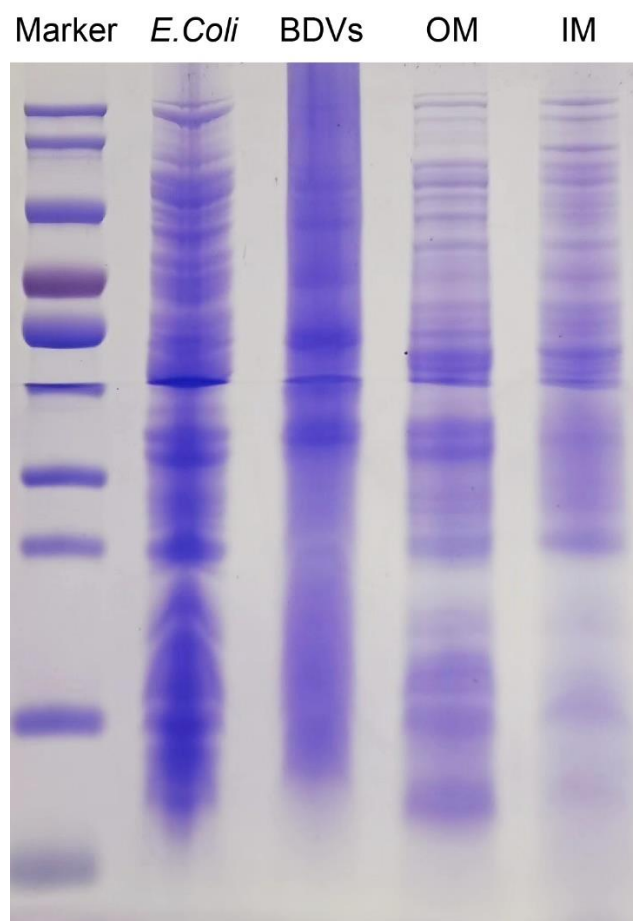
<sup>1</sup>These authors contributed equally to this work.

\*Corresponding author: Xudong Zhang, E-mail: zhangxd56@mail.sysu.edu.cn

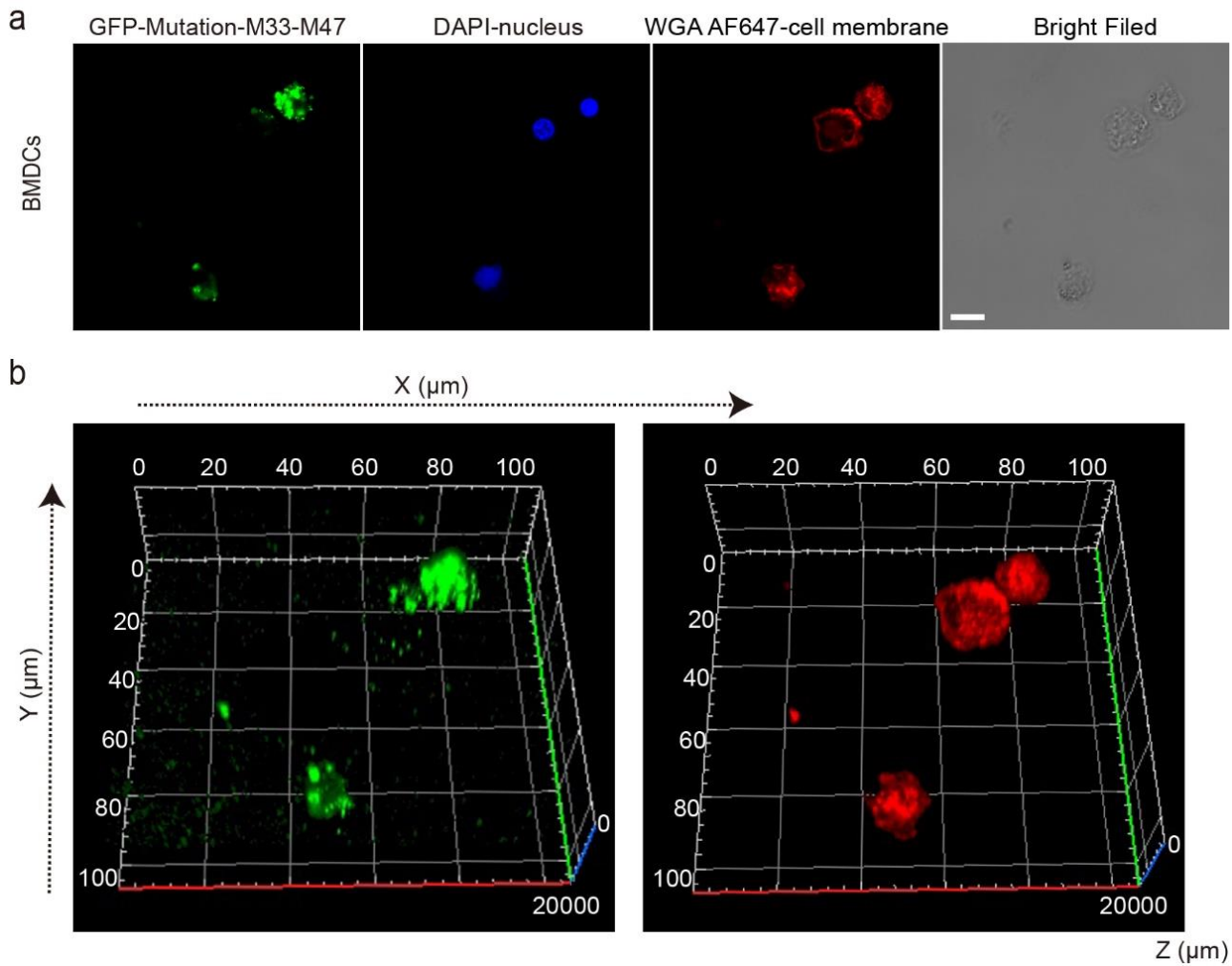
Xin Liang, E-mail: liangxingibh@gdmu.edu.cn



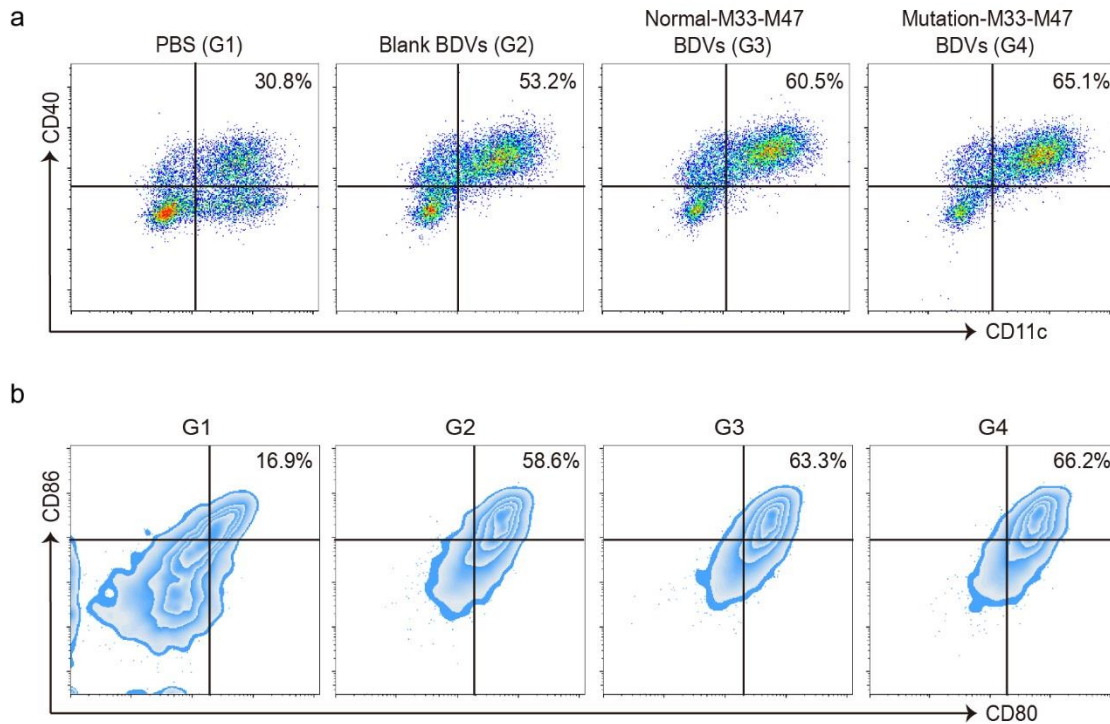
**Supplementary Figure 1.** Images of discontinuous sucrose density gradients post ultracentrifugation to separate the dual membranes of recombinant *E. coli* BL21(DE3)plysS cells.



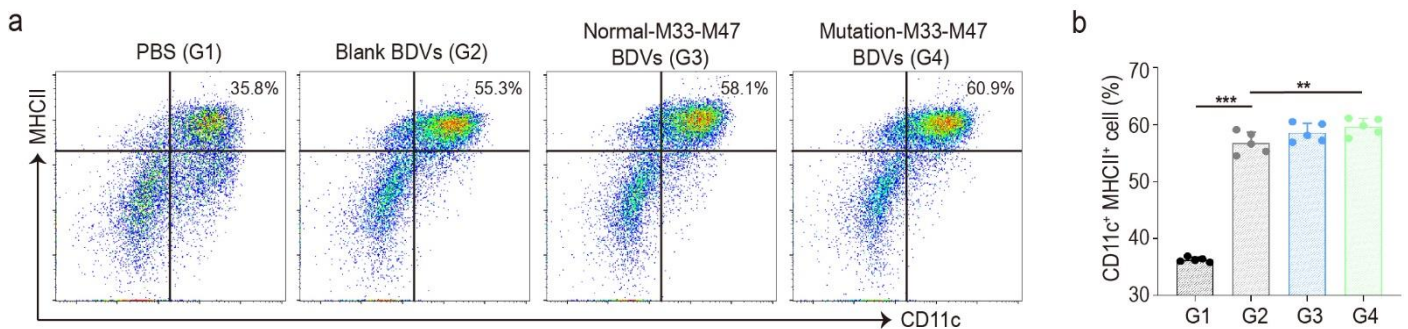
**Supplementary Figure 2.** SDS-polyacrylamide gel electrophoresis of *E. Coli*, **BDVs**, OM and IM.



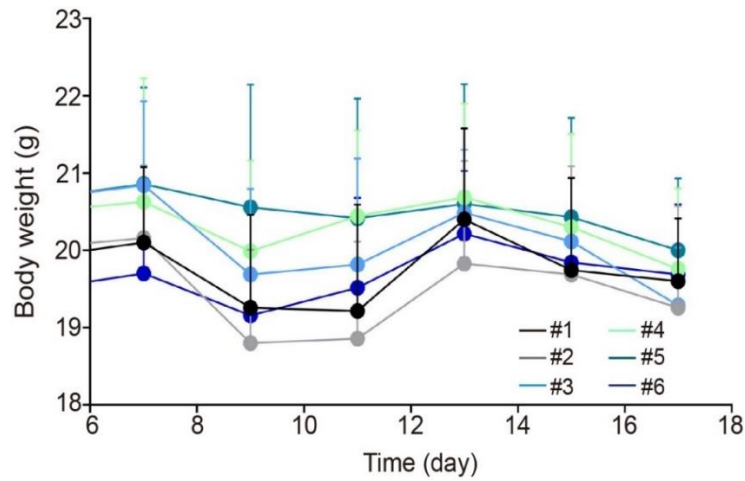
**Supplementary Figure 3. Dendritic cell maturation *in vitro*.** (a) Confocal image of BMDCs uptake of *E. coli* GFP-Mutation-M33-M47 **BDVs** *in vitro* (Scale bar: 10 μm). (b) Confocal 3D image of BMDCs uptake of *E. coli* GFP-Mutation-M33-M47 **BDVs** *in vitro*. Green: **BDVs**. Red: cell membrane. Blue: cell nucleus.



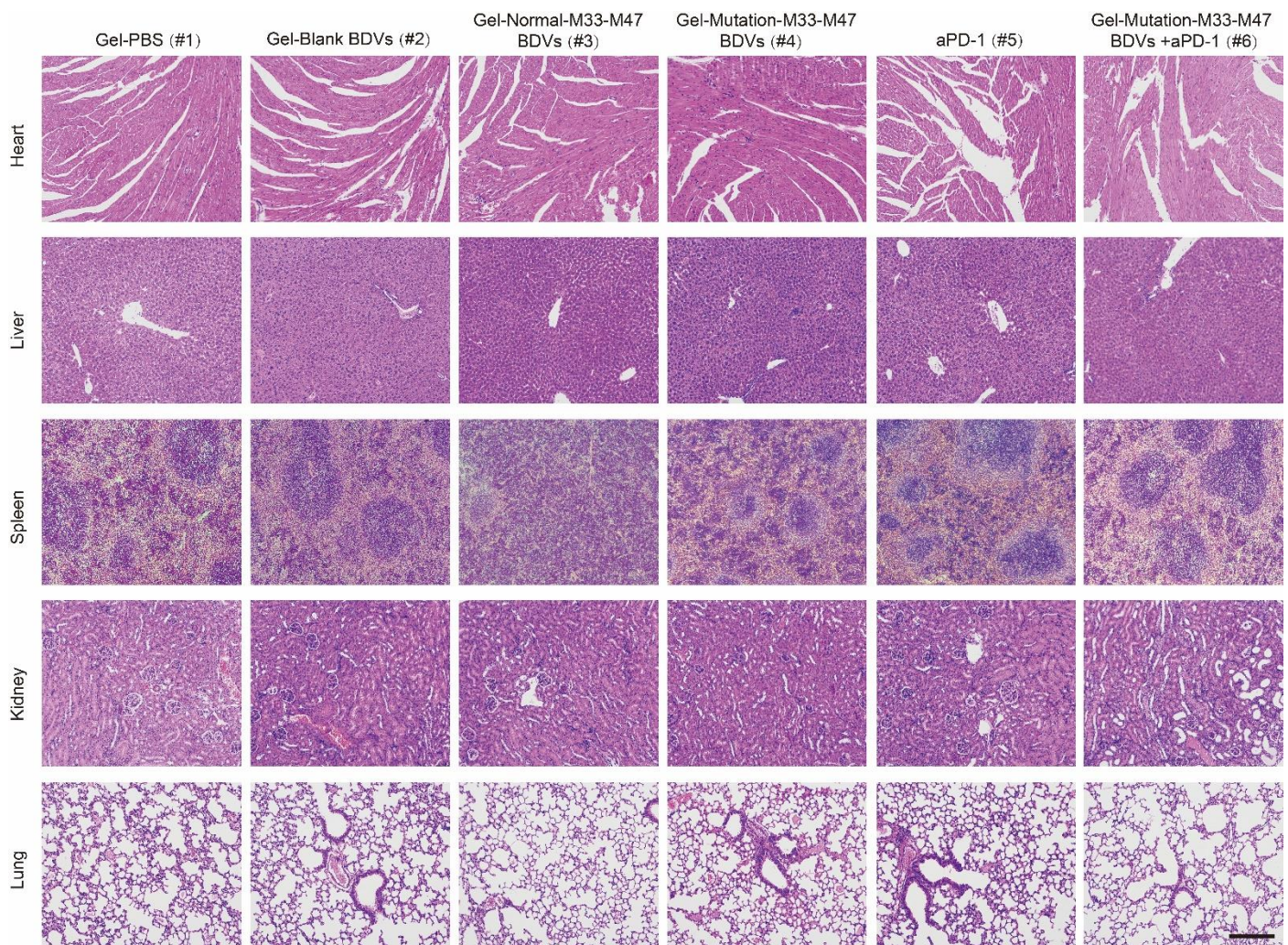
**Supplementary Figure 4.** Representative flow cytometry plots of CD11c<sup>+</sup> CD40<sup>+</sup> cells (a) and mature DCs (b) induced by different formulations of BDVs *in vitro* (gated on CD11c<sup>+</sup> cells). Cells were stained with anti-CD11c-APC and anti-CD40-PE (a) antibodies; anti-CD11c-APC, anti-CD80-FITC and anti-CD86-PE (b) antibodies (Biolegend), separately. Error bar, mean  $\pm$  s.e.m. (G1) PBS, (G2) Blank **BDVs**, (G3) Normal-M33-M47 **BDVs**, (G4) Mutation-M33-M47 **BDVs**.



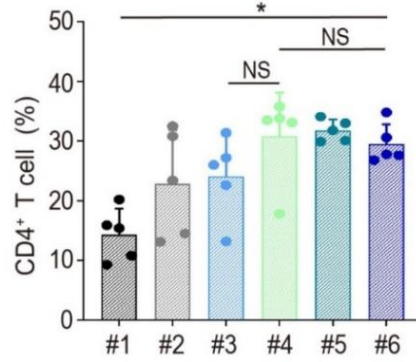
**Supplementary Figure 5.** Representative flow cytometry dot plots of CD11c<sup>+</sup> MHCII<sup>+</sup> cells (a) and statistical data (b) in different groups *in vitro* (gated on CD11c<sup>+</sup> cells,  $n = 5$ ). Cells were stained with anti-CD11c-APC, anti-mouse I-A/I-E-PE antibodies (Biolegend). Error bar, mean  $\pm$  s.e.m. \* $P < 0.05$ , \*\* $P < 0.01$ , \*\*\* $P < 0.001$ . One-way ANOVA with Tukey post-hoc tests (b).



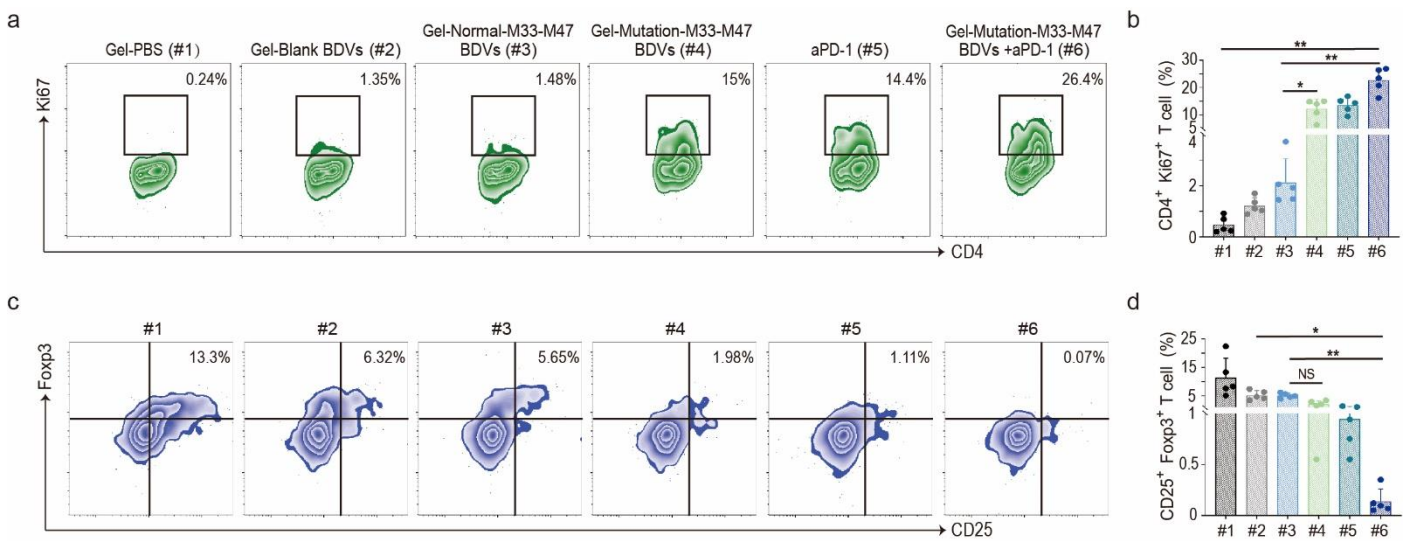
**Supplementary Figure 6.** Body weights of mice in different groups during treatment ( $n = 7$ ). (#1) Gel-PBS, (#2) Gel-Blank **BDVs**, (#3) Gel-Normal-M33-M47 **BDVs**, (#4) Gel-Mutation-M33-M47 **BDVs**, (#5) aPD-1, (#6) Gel-Mutation-M33-M47 **BDVs** + aPD-1. Error bar, mean  $\pm$  s.e.m..



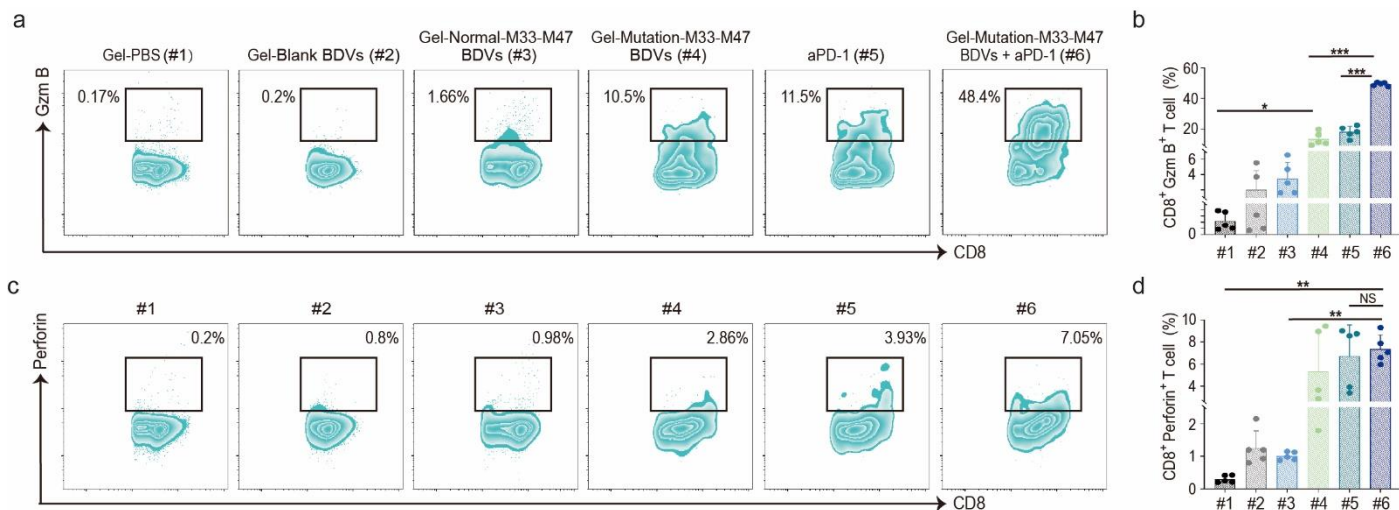
**Supplementary Figure 7.** The H&E staining histological images of heart, liver, spleen, kidney and lung of mice in different experimental groups. Scale bar: 100  $\mu$ m.



**Supplementary Figure 8.** Quantitative analysis of CD4<sup>+</sup> T cells from different treatment groups (gated on CD3<sup>+</sup> T cells,  $n = 5$ ). Error bar, mean  $\pm$  s.d.. (#1) Gel-PBS, (#2) Gel-Blank BDVs, (#3) Gel-Normal-M33-M47 BDVs, (#4) Gel-Mutation-M33-M47 BDVs, (#5) aPD-1, (#6) Gel-Mutation-M33-M47 BDVs + aPD-1.



**Supplementary Figure 9. a, b,** Representative flow cytometry plots (a) and ratios (b) of different groups of CD4<sup>+</sup> Ki67<sup>+</sup> T cells in tumors (gated on CD3<sup>+</sup> CD4<sup>+</sup> T cells,  $n = 5$ ). Cells were stained with anti-CD3-FITC, anti-CD4-PE, anti-Ki67-Alexa Fluor<sup>®</sup> 647 antibodies (Biolegend). Error bar, mean  $\pm$  s.d.. **c, d,** Representative flow cytometry plots and ratios of CD25<sup>+</sup> Foxp3<sup>+</sup> T cells in the tumors from different groups (Gated on CD3<sup>+</sup> CD4<sup>+</sup> T cells,  $n = 5$ ). Cells were stained with anti-CD4-PE, anti-CD25-Brilliant Violet 421, anti-Foxp3-Alexa Fluor<sup>®</sup> 647 antibodies (Biolegend). Error bar, mean  $\pm$  s.d.. (#1) Gel-PBS, (#2) Gel-Blank BDVs, (#3) Gel-Normal-M33-M47 BDVs, (#4) Gel-Mutation-M33-M47 BDVs, (#5) aPD-1, (#6) Gel-Mutation-M33-M47 BDVs + aPD-1. NS: no significant, \* $P < 0.05$ , \*\* $P < 0.01$ , \*\*\* $P < 0.001$ . One-way ANOVA with Tukey post-hoc tests (b, d).



**Supplementary Figure 10. a, b**, Representative flow cytometry plots (a) and ratios (b) of different groups of CD8<sup>+</sup> Gzm B<sup>+</sup> T cells in tumors (gated on CD3<sup>+</sup> CD8<sup>+</sup> T cells,  $n = 5$ ). Error bar, mean  $\pm$  s.d.. **c, d**, Representative flow cytometry plots and ratios of CD8<sup>+</sup> Perforin<sup>+</sup> T cells in the tumors from different groups (gated on CD3<sup>+</sup> CD8<sup>+</sup> T cells,  $n = 5$ ). Error bar, mean  $\pm$  s.d.. Cells were stained with anti-CD3-FITC, anti-CD8-APC/Fire750, anti-Granzyme B-PE, anti-Perforin-APC antibodies (Biolegend). (#1) Gel-PBS, (#2) Gel-Blank BDVs, (#3) Gel-Normal-M33-M47 BDVs, (#4) Gel-Mutation-M33-M47 BDVs, (#5) aPD-1, (#6) Gel-Mutation-M33-M47 BDVs + aPD-1. NS: no significant, \* $P < 0.05$ , \*\* $P < 0.01$ , \*\*\* $P < 0.001$ . One-way ANOVA with Tukey post-hoc tests (b and d).

**Supplementary Table 1.** Substitution sites are indicated by red letters and linker sequence is indicated by green letters.

Name	Nucleotide sequence (5'---3')
Normal-M33-M47	GACAGTGGAAGTCCTTTTCCAGCAGCTGTAATTCTCAGAGTTGCTTTGCACATGGC CAGAGGGCTAAAGTACCTGCACCAAGGCGGCGGCGGCAGCGGCGGCGGCGGCAG CGGCGGCGGCGGCAGCGGTCGAGGCCATCTCCTGGGCCGCCTGGCGGCCATCGTG GCTAAACAGGTAAGTCTGCTGGGCCGGAAGGTGGTGGTTCGTACGC
Mutation-M33-M47	GACAGTGGAAGTCCTTTTCCAGCAGCTGTAATTCTCAGAGATGCTTTGCACATGGC CAGAGGGCTAAAGTACCTGCACCAAGGCGGCGGCGGCAGCGGCGGCGGCGGCAG CGGCGGCGGCGGCAGCGGTCGAGGCCATCTCCTGGGCCGCCTGGCGGCCATCGTG GGTAAACAGGTAAGTCTGCTGGGCCGGAAGGTGGTGGTTCGTACGC